HHS Public Access

Author manuscript

J Neurooncol. Author manuscript; available in PMC 2015 November 17.

Published in final edited form as:

J Neurooncol. 2011 September ; 104(2): 579–587. doi:10.1007/s11060-011-0530-8.

A radiotherapy technique to limit dose to neural progenitor cell niches without compromising tumor coverage

Kristin J. Redmond,
Department of Radiation Oncology and Molecular Radiation Sciences, The Johns Hopkins University School of Medicine, 401 N Broadway, Suite 1440, Baltimore, MD 21231, USA

Pragathi Achanta,
Department of Neurosurgery, The Johns Hopkins University School of Medicine, Baltimore, MD, USA

Stuart A. Grossman,
Department of Oncology, The Johns Hopkins University School of Medicine, Baltimore, MD, USA

Michael Armour,
Department of Radiation Oncology and Molecular Radiation Sciences, The Johns Hopkins University School of Medicine, 401 N Broadway, Suite 1440, Baltimore, MD 21231, USA

Juvenal Reyes,
Department of Radiation Oncology and Molecular Radiation Sciences, The Johns Hopkins University School of Medicine, 401 N Broadway, Suite 1440, Baltimore, MD 21231, USA

Lawrence Kleinberg,
Department of Radiation Oncology and Molecular Radiation Sciences, The Johns Hopkins University School of Medicine, 401 N Broadway, Suite 1440, Baltimore, MD 21231, USA

Erik Tryggestad,
Department of Radiation Oncology and Molecular Radiation Sciences, The Johns Hopkins University School of Medicine, 401 N Broadway, Suite 1440, Baltimore, MD 21231, USA

Alfredo Quinones-Hinojosa, and
Department of Neurosurgery, The Johns Hopkins University School of Medicine, Baltimore, MD, USA

Eric C. Ford
Department of Radiation Oncology and Molecular Radiation Sciences, The Johns Hopkins University School of Medicine, 401 N Broadway, Suite 1440, Baltimore, MD 21231, USA

Eric C. Ford: eford6@jhmi.edu

Abstract

Radiation therapy (RT) for brain tumors is associated with neurocognitive toxicity which may be a result of damage to neural progenitor cells (NPCs). We present a novel technique to limit the

Correspondence to: Eric C. Ford, `eford6@jhmi.edu`.

Conflicts of interest Eric Ford, PhD and Erik Tryggestad, PhD are partially supported under a licensing agreement between the Johns Hopkins University and Gulmay Medical Ltd. for commercialization of the radiation devices discussed in this manuscript.

radiation dose to NPC without compromising tumor coverage. A study was performed in mice to examine the rationale and another was conducted in humans to determine its feasibility. C57BL/6 mice received localized radiation using a dedicated animal irradiation system with on-board CT imaging with either: (1) Radiation which spared NPC containing regions; (2) Radiation which did not spare these niches; or (3) Sham irradiation. Mice were sacrificed 24 h later and the brains were processed for immunohistochemical Ki-67 staining. For the human component of the study, 33 patients with primary brain tumors were evaluated. Two intensity modulated radiotherapy (IMRT) plans were retrospectively compared: a standard clinical plan and a plan which spares NPC regions while maintaining the same dose coverage of the tumor. The change in radiation dose to the contralateral NPC-containing regions was recorded. In the mouse model, non-NPC-sparing radiation treatment resulted in a significant decrease in the number of $Ki67^+$ cells in dentate gyrus (DG) ($P = 0.008$) and subventricular zone (SVZ) ($P = 0.005$) compared to NPC-sparing radiation treatment. In NPC-sparing clinical plans, NPC regions received significantly lower radiation dose with no clinically relevant changes in tumor coverage. This novel radiation technique should significantly reduce radiation doses to NPC containing regions of the brain which may reduce neurocognitive deficits following RT for brain tumors.

Keywords

Neural progenitor cells; Neural stem cell niches; Ki-67; Intensity modulated radiation therapy; Neurocognitive toxicity

Introduction

Radiation therapy (RT) is a critical component in the treatment of a wide variety of brain tumors. However, it is associated with significant toxicities to normal brain tissue. Numerous studies have demonstrated severe neurocognitive deficits following cranial irradiation, most notably in children [1–6]. The precise mechanism for this remains unclear and is likely multifactorial. Animal studies have shown an association between radiation-induced dysfunction of neural progenitor cells (NPCs) and neurocognitive decline following central nervous system irradiation, with effects seen at doses as low as 2 Gy [7, 8]. One hypothesis is that irradiation inhibits neurogenesis in the dentate gyrus (DG) [9]. This has been linked to behavioral changes in a number of animal studies [10–13].

NPCs are found in two regions of the adult mammalian brain: the subventricular zone (SVZ) of the lateral ventricles and the DG of the hippocampus [14–16]. These cells play an important role in repair of injury within the central nervous system [17, 18], including recovery from radiation induced damage [19, 20]. However, these cells are extremely sensitive to radiation as are their progenitor stem cell populations [7, 21–23]. Studies suggest that neurogenic areas similar to those described in the rodent brain exist in the human brain as well [16], and that injury to these regions may be contribute to the long term neurocognitive sequelae associated with cancer therapy. For example, intrathecal methotrexate in children receiving prophylactic therapy for acute lymphoblastic leukemia is known to cause long term neurotoxicity [24–27]. Since this cycle active drug penetrates only

a thin layer of tissue around the ventricles, it is likely that injury to cells in the periventricular region is related to long term cognitive deficits following this therapy [28].

In spite of the relationship between neurocognitive toxicity and injury to the NPCs, modern radiation treatment techniques do not attempt to limit the radiation dose to the NPC-containing niches. Three pilot studies each evaluating five or fewer patients suggest feasibility of ventricular or hippocampal-sparing RT [29–32]. However, no studies to date have assessed the feasibility of this approach in a population of patients with multiple different tumor volumes and geometries relative to the NPC containing niches. It is therefore unclear if radiation sparing of NPC regions is feasible in practice.

The purpose of this study was twofold: First, we delivered localized RT to rodents to assess whether conformal radiation techniques designed to spare the NPCs produced different results than conventional RT techniques. Second, we aimed to retrospectively examine the feasibility of using a simple modification to widely accepted radiation planning techniques to decrease the radiation dose to these progenitor cell containing areas without compromising radiation coverage of the tumor. The long term goal of this research approach is to minimize radiation injury to NPC containing regions of the brain and thereby hopefully reduce undesired neurocognitive outcomes in brain tumor survivors.

Materials and methods

NPC-sparing radiation in mice

Animals and radiation—The animal component of the study was conducted on 8 week old male C57BL/6 mice with the approval of the Johns Hopkins Animal Care and Use Committee under standard animal care and use protocols.

For radiation treatment planning purposes, a T2-weighted brain MRI of a 8 week old C57BL/6 mouse was acquired with a 9.4 T MRI BioSpec 94/20 (Bruker Inc., Billerica, MA) and was imported into the Pinnacle radiation treatment planning system (Philips Radiation Oncology Systems, Madison, WI). The MRI was used to contour the lateral ventricles and the capsule of the hippocampus.

Treatment with millimeter-scale radiation beams is performed using the small animal radiation research platform (SARRP), an in-house system with on-board CT imaging for guidance [33]. Animals were treated under anesthesia and immobilized using a stereotactic device. Two radiation treatment plans were developed to target a hypothetical tumor location in the cortex placed 1.5 mm lateral to the lateral ventricle. In the first plan (n = 3 mice), five 1 mm diameter non-coplanar X-ray beams were chosen to avoid the ispilateral ventricles and hippocampus using the 3D beams-eye view. In the second plan (n = 3 mice) five non-coplanar beams were evenly spaced with no intention of sparing the ipsilateral neural progenitor containing regions. Both plans used equally-weighted beams at a specified depth for a total intended dose of 20 Gy to the hypothetical target. The dose rate was approximately 1 Gy/min.

To quantify radiation dose distributions, Monte Carlo calculations were performed using the EGSnrc package [34] using CT images from the SARRP coregistered to the MRI images described above. BEAM was used to fully characterize the SARRP X-ray source and beam collimation devices. 225 kVp X-rays emitted from the 1 mm SARRP collimator were then tracked through the CT dataset using DOSXYZ, which accounts for tissue heterogeneity by mapping CT numbers to a set of predefined compounds (e.g., tissue and bone) with density ranges for each [35]. These calculations were carried out at a voxel resolution of 0.34 × 0.34 × 0.34 cubic mm. Resulting dose deposition grids were re-imported into the Pinnacle radiation planning system for display and quantitative evaluation. Dose volume histograms (DVH) for the structures of interest were calculated.

For precise targeting of the isocenter during treatment, an intrathecal iodine contrast injection was used to visualize the lateral ventricles on CT. The technique consisted of exposing the cisterna magna by moving three layers of muscle in the back of the neck, a sterile procedure performed under anesthesia and with the use of analgesics. Iodine contrast media, Iohexol 300 mgI/ml (GE Inc., Oslo, Norway), was injected under the dura mater, the thin membrane layer covering the cisterna magna using a 30 gauge needle on a 1 ml syringe. Injected volumes were 50 μl for a 13–20 g mouse and 70 μl for a 20–30 g mouse determined empirically to be non-toxic. The injection was performed with the aid of a microscope in order to ensure that the vessels lining the dorsal surface of the nervous system were not ruptured. The needle was held in place for 1 min to prevent backflow.

Radiation treatments were administered using 225 kVp, 13 mA, and 0.25 mm copper filtration on the SARRP under CT guidance. Five beams each of 1 mm diameter were delivered as outlined above. A third group of mice (n = 3) underwent sham irradiation, following all of the above described steps precisely, except that no radiation treatment was given.

Immunohistochemistry and stereologic counting—Twenty-four hours after radiation, the animals were sacrificed using transcardial perfusion under deep anesthesia first with 0.9% saline followed by 4% PFA. Brains were extracted and post-fixed for 8 h in PFA followed by a sink in 30% sucrose. Finally, the tissue was frozen in OCT. Cyrosectioning of coronal slices was performed at 10 μm slice thickness.

The marker for proliferation employed is Ki-67 which is a protein present in every phase of the cell cycle except G0 [36]. This marker has been widely used in studies of NPCs [8]. Immunohistochemical staining with Ki-67 was as follows: antigen retrieval with citric acid (0.01 M in deionized water), rinse in phosphate buffer solution (PBS, 3 × 5 min), 30 min in blocking serum (10% goat serum with 0.1% triton-X for membrane permeabilization), overnight incubation in rabbit monoclonal anti Ki-67 primary antibody at 4°C (1:200, Neomarkers), PBS rinse (3 × 5 min), 1 h in secondary antibody. The secondary antibody was conjugated with a fluorphor, 1:500 goat anti-mouse alexa fluor 488 conjugated (Millipore, Inc.) and nuclear stain with DAPI (4′-6-diamidino-2-phenylindole).

Stereological counting was performed using 10 μm tissue sections evenly spaced along the rostral-caudal length of the ipsilateral SVZ and DG. Cells were counted on every tenth

section. Because the radiation was planned without any intention of sparing the contralateral NPC containing niches, cell counting was not performed on the contralateral SVZ and DG of the brain.

Statistical analysis—A one-way ANOVA was performed using SigmaStat Software (version 3.1) to compare the number of Ki-67+ cells in the brains of animals treated with the NPC-sparing radiation, non-NPC-sparing radiation, and sham irradiation. Post hoc multiple comparisons using Student–Newman–Keuls method were used to determine significant differences between the groups.

Clinical feasibility

Thirty-three patients treated with intensity modulated radiotherapy (IMRT) for primary brain tumors at Johns Hopkins Hospital between August 2006 and February 2009 were selected at random and retrospectively evaluated in this study (Table 1). Approval was granted by the Johns Hopkins Hospital Institutional Review Board prior to data collection. Patients underwent a CT with contrast of the whole brain for treatment planning purposes using the Brilliance Big Bore CT simulator (Philips Inc., Cleveland, OH). In addition, all patients had pre-treatment MRI scans of the brain using a T1-weighted sequence with a gadolinium contrast agent and a FLAIR sequence which were manually co-registered with the planning CT for precise tumor delineation in the Pinnacle treatment planning system (v. 8.0m, Philips Inc., Madison, WI).

The planning target volume (PTV) for each patient was designated by the treating physician at the time of initial treatment planning. The margins reflect the institutional standard at the Johns Hopkins Hospital during the study period, and PTV contours were not modified in any way for the purpose of this study. NPC-containing niches were contoured on the T1-weighted MRI scan with gadolinium contrast and were defined as 5 mm region adjacent to the lateral wall of the lateral ventricle and the entire DG of the hippocampus.

The IMRT treatment plan used clinically for each patient was considered as a baseline plan. The PTV as defined on the initial IMRT plan was not modified in any way for the NPC-sparing IMRT plan. The NPC containing regions were defined as a 5 mm region adjacent to the lateral wall of the lateral ventricle as well as the entire hippocampus. A second IMRT plan using the NPC-containing regions of the brain as avoidance structures was created for each patient. In cases where the NPC-containing regions of the brain were encompassed by the PTV, additional contours were drawn such that modified avoidance structures only contained areas outside of the PTV in which sparing was believed to be possible. Inverse planning objective functions were identical between the initial and NSC sparing plans except for the addition of NPC containing regions as avoidance structures using maximum DVH criteria. Standard dose constraints to adjacent normal tissues were employed and were not modified from the institutional standard at the Johns Hopkins Hospital. Multiple iterations were made until the plan was maximally optimized such that further reductions in dose to the NPC containing regions resulted in reduction of tumor coverage. Final analysis of radiation dose to the NPC containing regions of the brain was based on the original complete contours rather than on the modified NPC contours drawn for planning purposes.

The dose to 70% or more of the volume (D70) was recorded for the right and left lateral wall of the lateral ventricle, right and left DG, and PTV for both the clinical and NPC-sparing IMRT plans for each patient. The absolute difference and percent change in D70 between the initial and NSC sparing plan was calculated for each structure.

Results

NPC-sparing radiation in mice

Dosimetry—Monte Carlo calculations confirmed that the NPC-sparing radiation plan delivered a lower radiation dose to the bilateral lateral ventricles and DG than the non-NPC-sparing radiation plan. Figure 1a–c and f–h shows MRI and CT images from the mouse radiation treatment plans showing the Monte-Carlo-based radiation dose distributions for the non-NPC sparing and NPC-sparing radiation treatment plans. In the non-NPC sparing plan, the region of the SVZ along the ipsilateral lateral ventricle receives a high radiation dose as does the ipsilateral DG, whereas the dose to these regions are substantially reduced in the NPC-sparing radiation treatment plan. Table 2 shows the mean doses to the NPC-containing niches for both the NPC-sparing and non-NPC sparing radiation plans.

Ki-67 staining—Figure 1d and e shows Ki-67 staining from a mouse receiving non-NPC sparing RT. By contrast, Fig. 1i and j shows Ki-67 staining from a mouse receiving NPC-sparing radiation. The Ki-67+ cells in the SVZ of the lateral ventricles are clearly visible. There is a qualitative decrease in the number of Ki-67+ cells in the non-NPC sparing radiotherapy plan compared with the NPC-sparing radiotherapy plan. Stereologic counting was used to quantify the difference in Ki-67+ cells in the ipsilateral NPC-containing regions between mice treated with the NPC-sparing radiation plan, non-NPC-sparing radiation plan, and sham irradiation. Figure 2a and b shows the mean number of Ki-67+ cells in the SVZ and DG, respectively, of each treatment group. Multiple comparisons using the Student–Newman–Keuls method showed a significant decrease in number of Ki-67+ cells in the ipsilateral DG ($P = 0.008$) and SVZ ($P = 0.005$) of animals treated with the NPC-sparing versus non-sparing plans. There was no difference in the number of Ki-67+ cells in the ipsilateral DG ($P = 0.068$) and the SVZ ($P = 0.810$) of animals treated with NPC-sparing radiation versus sham irradiation.

Clinical feasibility

Figure 3 shows IMRT plans for a patient with GBM in the left tempoparietal lobe. The NPC-sparing radiotherapy plan (right) reduces the radiation dose to a portion of the

Figure 4 shows the DVH from the clinical IMRT plan (dashed line) compared with the DVH from the NPC-sparing IMRT plan (solid line) for a patient with GBM. Note that there is no clinically relevant change in coverage of the tumor PTV, but there is marked reduction of dose to the contralateral SVZ. The ipsilateral SVZ and ipsilateral DG (not shown) are contained within the target volume and therefore receive full dose in both plans.

In IMRT plans, the mean improvement in dose received by 70% (D70) of the contralateral DG is greater than 30% in patients with GBM and less in other histologies. The mean improvement in D70 to the contralateral lateral ventricle is greater than 60% in patients with

pituitary adenoma and less in other histologies. Table 3 shows the improvement in D70 to the contralateral DG in the NPC-sparing IMRT plan compared with the initial IMRT plan, and improvement in D70 to the contralateral lateral wall of the lateral ventricle in the NPC sparing IMRT plan compared with the initial IMRT plan for each tumor histology. By design, decreases in dose to the NPC containing regions were associated with no clinically relevant change in dosimetric coverage of the PTV.

Discussion

RT is an integral component of the treatment of tumors of the central nervous system, but the long term neurocognitive toxicity associated with radiation to the brain can be severe and have important negative consequences on patient quality of life. Numerous animal studies have demonstrated a relationship between radiation dose to the NPC-containing niches and neurocognitive decline following RT [7, 8]. Although modern RT techniques such as IMRT allow radiation oncologists to precisely target and deliver radiation to at-risk areas of the brain while sparing critical adjacent normal structures, currently no effort is made to limit radiation dose to the NPC-containing SVZ of the lateral ventricle or the DG of the hippocampus. We propose a simple modification of the standard of care RT for brain tumors with minimal associated risks, but the potential to improve cognitive function and quality of life in brain tumor survivors.

Our animal model demonstrates that focal NPC-sparing radiation techniques effectively spare proliferating cells at 24 h after radiation. This is the first study to our knowledge to demonstrate that conventional radiation techniques result in a significant decrease in proliferative cells compared to NPC-sparing radiation techniques. Our human feasibility data demonstrate that it is possible to spare a portion of the SVZ of the lateral ventricles and the hippocampus using IMRT in a population of patients with a wide variety of tumor geometries and locations relative to the NPC-containing niches. This sparing is possible without modifying the original target volume and without any clinically relevant change in dosimetric coverage of the tumor.

The concept of neural stem cell-sparing RT was previously presented by Barani et al. [31] utilizing a single patient CT dataset to generate conventional and NPC sparing radiation treatment plans for two theoretical clinical scenarios: (1) A case of brain metastases in which they compared whole brain RT using opposed lateral radiation beams with an IMRT plan to treat the whole brain volume; (2) A high-grade glioma in which they compared a standard three-field technique using opposed laterals plus an anterior superior oblique beam with an IMRT field. Similarly, Ghia et al. [29] performed an exploratory analysis in a single patient which suggested that it is possible to selectively boost visible brain metastases while avoiding the hippocampus when treating brain metastases with whole brain RT. Gondi et al. [32] recently published a detailed description of their hippocampal-sparing whole brain RT technique in preparation for testing neurocognitive outcomes in a cooperative group trial.

Our NPC-sparing RT technique differs from the prior studies. Rather than trying to limit the radiation dose to the NPC regions globally, we attempt to create a cold spot within some region of the NPC-containing niche in which we apply very tight dose constraints to a

limited volume. The purpose is to restrict the radiation dose to this region to a level that will truly spare the cells, to allow these cells to assist with repair throughout the brain. Another important distinction from Gondi et al. [32] is that we aim to spare the NPC within SVZ, as possible, whereas they attempt to spare the hippocampus alone. Furthermore, our human planning data represent an important expansion of the previous studies as our analysis shows that NPC-sparing RT is feasible in more than 30 patients.

There are several limitations to this study. First, the radiation tolerance of the NPC to fractionated RT using IMRT delivery remains to be elucidated. Some investigators have speculated that the dose tolerance of NPC containing regions may be 10–20 Gy with variation based on fraction size, however at present the dose tolerance and volume effect of NPC sparing in humans remains uncertain. Animal studies are ongoing in our laboratory to answer this question. Second, although limited studies suggest that neurogenic niches are comparable in humans as in rodents [16], the details remain to be investigated. Third, our mouse experiments were limited to the assessment of Ki-67+ cells at a relatively early time point (24 h). Though this is a standard approach applied previously in NPC studies [8], our experiment is different in that we deliver a different overall dose at a different dose rate. Future studies will be important to assess the impact of local radiation on survival and differentiation at both earlier and later time points as well as the impact of this change on neurocognitive outcomes. Additional studies will also be important in order to obtain a longer window of evaluation and to explore the impact of dose escalation.

In conclusion, we propose a novel RT technique in which modern standard-of-care radiation treatment planning technology is used to spare the NPC-containing niches of the brain without compromising tumor coverage. We used a mouse model to demonstrate that the NPC-sparing RT technique effectively spares NPCs at an early time point and performed a retrospective human planning study to demonstrate that NPC-sparing is feasible in a large number of brain tumor patients with a wide variety of tumor locations and geometries relative to the NPC-containing niches. We believe this technique may represent a method to reduce long term neurocognitive toxicity following RT for brain tumors without additional costs or added risks for the patient.

Acknowledgments

Grant support: Alfredo Quinones-Hinojosa, MD NIH/NINDS K08, HHMI, The Robert Wood Johnson Foundation/ Harold Amos Medical Faculty Development Program, Maryland Stem Cell Technology Development Corporation (TEDCO), Children Cancer Foundation (CCF).

References

1. Johannesen TB, Lien HH, Hole KH, Lote K. Radiological and clinical assessment of long-term brain tumour survivors after radiotherapy. Radiother Oncol. 2003; 69(suppl 2):169–176. [PubMed: 14643954]
2. Silber JH, Radcliffe J, Peckham V, et al. Whole-brain irradiation and decline in intelligence: the influence of dose and age on IQ score. J Clin Oncol. 1992; 10(suppl 9):1390–1396. [PubMed: 1517781]
3. Ris MD, Packer R, Goldwein J, Jones-Wallace D, Boyett JM. Intellectual outcome after reduced-dose radiation therapy plus adjuvant chemotherapy for medulloblastoma: a children's cancer group study. J Clin Oncol. 2001; 19(suppl 15):3470–3476. [PubMed: 11481352]

4. Hoppe-Hirsch E, Brunet L, Laroussinie F, et al. Intellectual outcome in children with malignant tumors of the posterior fossa: influence of the field of irradiation and quality of surgery. Childs Nerv Syst. 1995; 11(suppl 6):340–346. [PubMed: 7671269]
5. Schatz J, Kramer JH, Ablin A, Matthay KK. Processing speed, working memory, and IQ: a developmental model of cognitive deficits following cranial radiation therapy. Neuropsychology. 2000; 14(suppl 2):189–200. [PubMed: 10791859]
6. Penitzka S, Steinvorth S, Sehlleier S, Fuß M, Wannenmacher M, Wenz F. Assessment of cognitive functions after prophylactic and therapeutic whole brain irradiation using neuropsychological testing. Strahlenther Onkol. 2002; 178(suppl 5):252–258. [PubMed: 12082684]
7. Tada E, Parent JM, Lowenstein DH, Fike JR. X-irradiation causes a prolonged reduction in cell proliferation in the dentate gyrus of adult rats. Neuroscience. 2000; 99(suppl 1):33–41. [PubMed: 10924950]
8. Mizumatsu S, Monje ML, Morhardt DR, Rola R, Palmer TD, Fike JR. Extreme sensitivity of adult neurogenesis to low doses of X-irradiation. Cancer Res. 2003; 63(suppl 14):4021–4027. [PubMed: 12874001]
9. Monje ML, Toda H, Palmer TD. Inflammatory blockade restores adult hippocampal neurogenesis. Science. 2003; 302(suppl 5651):1760–1765. [PubMed: 14615545]
10. Madsen TM, Kristjansen PEG, Bolwig TG, Wörtwein G. Arrested neuronal proliferation and impaired hippocampal function following fractionated brain irradiation in the adult rat. Neuroscience. 2003; 119(suppl 3):635–642. [PubMed: 12809684]
11. Rola R, Raber J, Rizk A, et al. Radiation-induced impairment of hippocampal neurogenesis is associated with cognitive deficits in young mice. Exp Neurol. 2004; 188(suppl 2):316–330. [PubMed: 15246832]
12. Saxe MD, Battaglia F, Wang J, et al. Ablation of hippo-campal neurogenesis impairs contextual fear conditioning and synaptic plasticity in the dentate gyrus. Proc Natl Acad Sci USA. 2006; 103(suppl 46):17501–17506. [PubMed: 17088541]
13. Winocur G, Wojtowicz JM, Sekeres M, Snyder JS, Wang S. Inhibition of neurogenesis interferes with hippocampus-dependent memory function. Hippocampus. 2006; 16(suppl 3):296–304. [PubMed: 16411241]
14. Gage FH. Mammalian neural stem cells. Science. 2000; 287(suppl 5457):1433–1438. [PubMed: 10688783]
15. Quinones-Hinojosa A, Sanai N, Soriano-Navarro M, et al. Cellular composition and cytoarchitecture of the adult human subventricular zone: a niche of neural stem cells. J Comp Neurol. 2006; 494(suppl 3):415–434. [PubMed: 16320258]
16. Sanai N, Tramontin AD, Quinones-Hinojosa A, et al. Unique astrocyte ribbon in adult human brain contains neural stem cells but lacks chain migration. Nature. 2004; 427(suppl 6976):740–744. [PubMed: 14973487]
17. Arvidsson A, Collin T, Kirik D, Kokaia Z, Lindvall O. Neuronal replacement from endogenous precursors in the adult brain after stroke. Nat Med. 2002; 8(suppl 9):963–970. [PubMed: 12161747]
18. Goings GE, Sahni V, Szele FG. Migration patterns of subventricular zone cells in adult mice change after cerebral cortex injury. Brain Res. 2004; 996(suppl 2):213–226. [PubMed: 14697499]
19. François S, Bensidhoum M, Mouiseddine M, et al. Local irradiation not only induces homing of human mesenchymal stem cells at exposed sites but promotes their widespread engraftment to multiple organs: a study of their quantitative distribution after irradiation damage. Stem Cells. 2006; 24(suppl 4):1020–1029. [PubMed: 16339642]
20. Mouiseddine M, François S, Semont A, et al. Human mesenchymal stem cells home specifically to radiation-injured tissues in a non-obese diabetes/severe combined immunodeficiency mouse model. Br J Radiol. 2007; 80(suppl SPEC ISS 1):S49–S55. [PubMed: 17704326]
21. Fike JR, Rola R, Limoli CL. Radiation response of neural precursor cells. Neurosurg Clin N Am. 2007; 18(suppl 1):115–127. [PubMed: 17244559]
22. Panagiotakos G, Alshamy G, Chan B, et al. Long-term impact of radiation on the stem cell and oligodendrocyte precursors in the brain. PLoS ONE. 2007; 2(suppl 7):e588. [PubMed: 17622341]

23. Hopewell JW, Cavanagh JB. Effects of X irradiation on the mitotic activity of the subependymal plate of rats. Br J Radiol. 1972; 45(suppl 534):461–465. [PubMed: 5029031]
24. Iuvone L, Mariotti P, Colosimo C, Guzzetta F, Ruggiero A, Riccardi R. Long-term cognitive outcome, brain computed tomography scan, and magnetic resonance imaging in children cured for acute lymphoblastic leukemia. Cancer. 2002; 95(suppl 12):2562–2570. [PubMed: 12467071]
25. Lesnik PG, Ciesielski KT, Hart BL, Benzel EC, Sanders JA. Evidence for cerebellar-frontal subsystem changes in children treated with intrathecal chemotherapy for leukemia: enhanced data analysis using an effect size model. Arch Neurol. 1998; 55(suppl 12):1561–1568. [PubMed: 9865801]
26. Waber DP, Tarbell NJ, Kahn CM, Gelber RD, Sallan SE. The relationship of sex and treatment modality to neuropsychologic outcome in childhood acute lymphoblastic leukemia. J Clin Oncol. 1992; 10(suppl 5):810–817. [PubMed: 1569453]
27. Bakke SJ, Fossen A, Storm-Mathiesen I, Lie SO. Long-term cerebral effects of CNS chemotherapy in children with acute lymphoblastic leukemia. Pediatr Hematol Oncol. 1993; 10(suppl 3):267–270. [PubMed: 8217544]
28. Grossman SA, Reinhard CS, Loats HL. The intracerebral penetration of intraventricularly administered methotrexate: a quantitative autoradiographic study. J Neurooncol. 1989; 7(suppl 4): 319–328. [PubMed: 2585028]
29. Ghia A, Tomé WA, Thomas S, et al. Distribution of brain metastases in relation to the hippocampus: implications for neurocognitive functional preservation. Int J Radiat Oncol Biol Phys. 2007; 68(suppl 4):971–977. [PubMed: 17446005]
30. Gutiérrez AN, Westerly DC, Tomé WA, et al. Whole brain radiotherapy with hippocampal avoidance and simultaneously integrated brain metastases boost: a planning study. Int J Radiat Oncol Biol Phys. 2007; 69(suppl 2):589–597. [PubMed: 17869672]
31. Barani IJ, Cuttino LW, Benedict SH, et al. Neural stem cell-preserving external-beam radiotherapy of central nervous system malignancies. Int J Radiat Oncol Biol Phys. 2007; 68(suppl 4):978–985. [PubMed: 17467925]
32. Gondi V, Tollakanahalli R, Mehta M, et al. Hippocampal-sparing whole brain radiotherapy: a “how-to” technique using helical tomotherapy and linear accelerated based intensity-modulated radiotherapy. Int J Radiat Oncol Biol Phys. 2010; 78(4):1244–1252. [PubMed: 20598457]
33. Wong J, Armour E, Kazanzides P, et al. High-resolution, small animal radiation research platform with X-ray tomographic guidance capabilities. Int J Radiat Oncol Biol Phys. 2008; 71(suppl 5): 1591–1599. [PubMed: 18640502]
34. Tryggestad E, Armour M, Iordachita I, Verhaegen F, Wong JW. A comprehensive system for dosimetric commissioning and Monte Carlo validation for the small animal radiation research platform. Phys Med Biol. 2009; 54(suppl 17):5341–5357. [PubMed: 19687532]
35. Rogers DWO, Faddegon BA, Ding GX, Ma C, We J, Mackie TR. BEAM: a Monte Carlo code to simulate radiotherapy treatment units. Med Phys. 1995; 22(suppl 5):503–524. [PubMed: 7643786]
36. Kee N, Sivalingam S, Boonstra R, Wojtowicz JM. The utility of Ki-67 and BrdU as proliferative markers of adult neurogenesis. J Neurosci Methods. 2002; 115(suppl 1):97–105. [PubMed: 11897369]

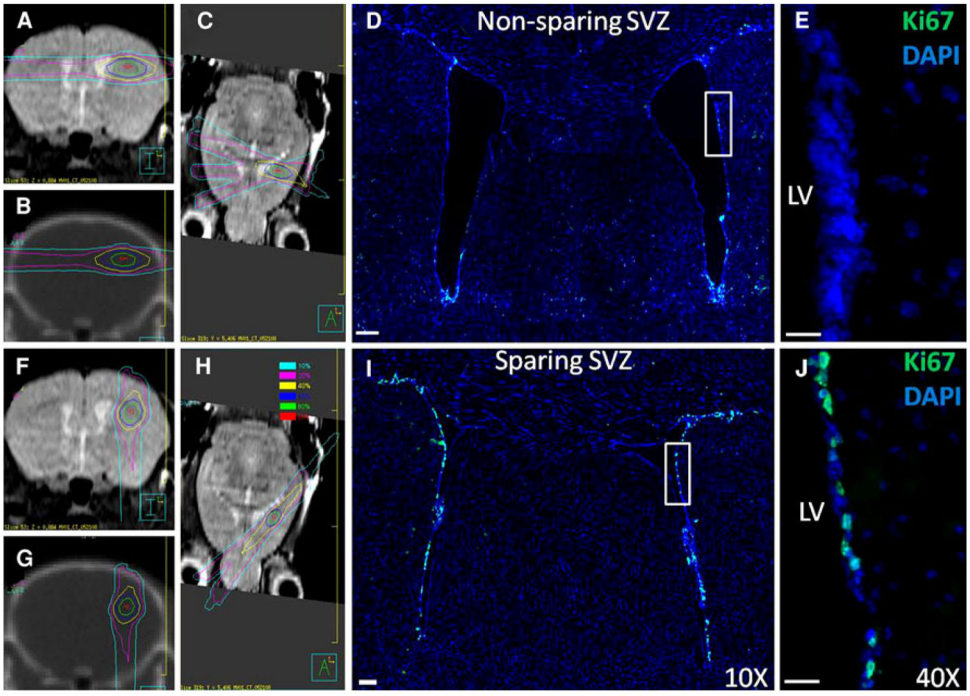

Fig. 1.

Mouse radiation treatment plans (*left*) and microscopy images (*right*) for the non-NPC-sparing (*top*) and NPC-sparing (*bottom*) radiotherapy plans. *Left side* MRI and CT images from the mouse radiation treatment plans showing the radiation dose distribution for the non-NPC sparing (*top*; **a–c**) and NPC-sparing radiation treatment plans (*bottom*; **f–h**). Note that for the non-NPC sparing plan, the region of the SVZ of the ipsilateral lateral ventricle receives a high radiation dose, whereas this region is effectively spared in the NPC Scans are: coronal MRI (**a**, **f**), coronal CT (**b**, **g**), and axial MRI (**c**, **h**). Dose values are shown in the legend. *Right side* Coronal sections showing Ki-67 stains (*green*) in the SVZ of the lateral ventricles following non-NPC sparing RT (**d**, **e**) and NPC-sparing RT (**i**, **j**). Co-staining is with DAPI (*blue*). Images **d** and **i** were taken with a 10× objective and the images e and **j** with 40× objective. *LV* left ventricle. (Color figure online)

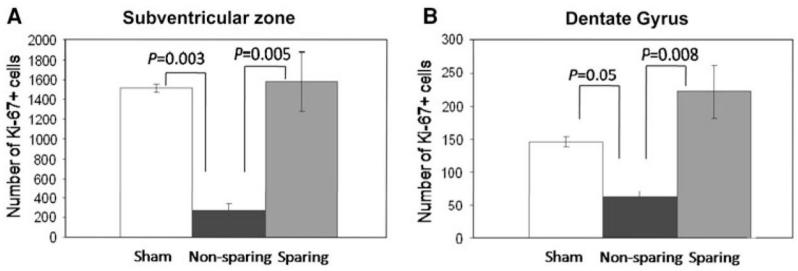

Fig. 2.

Ki67+ cell counts for three irradiation schemes: sham irradiation (*white*), non-NPC sparing radiation (*black*), and NPC-sparing radiation (*gray*) in the ipsilateral SVZ (**a**) and DG (**b**). There is no significant difference between the sham irradiation and NPC-sparing radiation groups

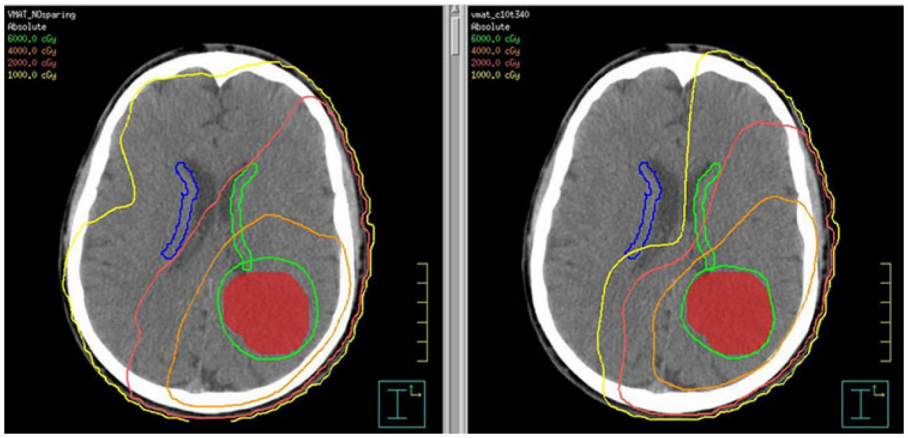

Fig. 3.

Example radiotherapy plan from a patient with GBM showing the tumor (*red*) and *solid lines* delineating the isodose distribution (region of brain receiving a given dose of radiation). The *left image* is an axial slice from the non-NPC-sparing plan and the *right image* is from an NPC-sparing plan showing that a portion of the contralateral SVZ (*blue*) is limited to <5 Gy (*light green isodose line*) and the majority is limited to <10 Gy (*yellow isodose line*). Isodose lines are as follows: *green* 60 Gy, *orange* 40 Gy, *red* 20 Gy, *yellow* 10 Gy, *light green* 5 Gy. (Color figure online) contralateral SVZ region compared to the standard plan (left) without compromising tumor coverage.

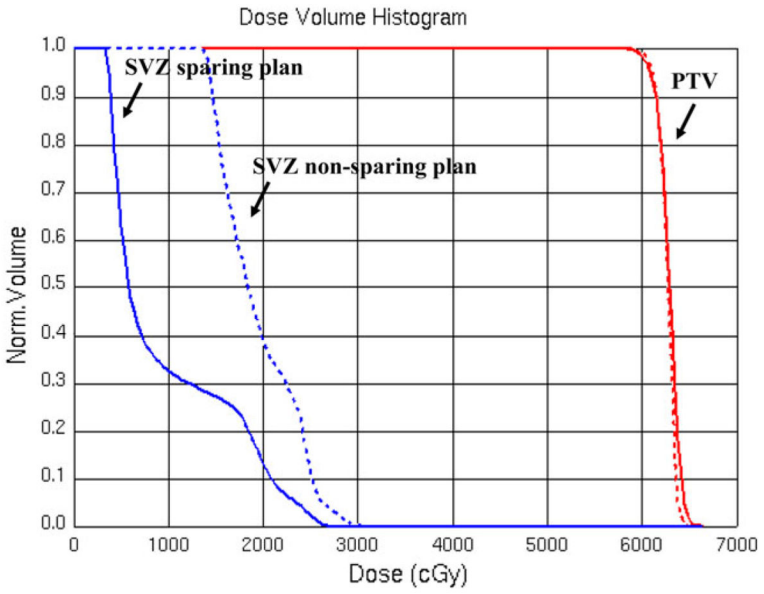

Fig. 4.

Example DVH for patient with GBM, showing the volume of the region (*Y*-axis) receiving less than or equal to a given dose of radiation (*X*-axis). *Dashed lines* represent the non-NPC-sparing plan. The *solid lines* represent the NPC-sparing radiation plan. *Blue* Contralateral SVZ. *Red* planning target volume (PTV = tumor plus margin). Note that close to 100% of the PTV is receiving the prescription radiation dose of 60 Gy in both the NPC-sparing and non-NPC-sparing RT plans, but that there is a substantial reduction in the radiation dose to the contralateral SVZ in the NPC-sparing RT plan compared with the non-NPC sparing RT plan. (Color figure online)

Table 1

Patient characteristics

Patient	Gender	Initial dose (Gy)	Extent of surgery	Histology	Tumor location
G1	Female	46	STR	GBM	Left parietal
G2	Female	46	STR	GBM	Left frontotemporal
G3	Female	46	STR	GBM	Left temporal
G4	Male	46	GTR	GBM	Left temporal
G5	Male	46	STR	GBM	Left temporal
G6	Male	46	STR	GBM	Right frontal
G7	Female	46	STR	GBM	Right temporal
G8	Male	46	GTR	GBM	Left parietal
G9	Female	46	GTR	GBM	Left temporal
G10	Female	46	GTR	GBM	Left temporal
L1	Female	45	GTR	Grade 2 astrocytoma	Right parietotemporal
L2	Female	45	GTR	Grade 2 oligodendroglioma	Left temporal
L3	Female	45	STR	Grade 2 oligoastrocytoma	Right temporal
L4	Male	45	STR	Grade 2 astrocytoma	Left frontoparietal
L5	Male	45	STR	Grade 2 astrocytoma	Right temporal
L6	Male	45	Biopsy	Grade 2 astrocytoma	Right frontal
L7	Male	45	STR	Tectal glioma	Tectum
L8	Male	45	GTR	Grade 2 astrocytoma	Right frontotemporal
L9	Male	45	GTR	Grade 2 oligoastrocytoma	Left frontal
L10	Female	45	STR	Low grade oligodendroglioma	Right frontoparietotemporal
M1	Female	50.4	Biopsy	Benign meningioma	Right cavernous sinus
M2	Female	50.4	STR	Benign meningioma	Right suprasellar region
M3	Male	52.2	STR	Benign meningioma	Left suprasellar region
M4	Female	52.2	STR	Benign meningioma	Left retro-orbital region to skull base
M5	Female	50.4	STR	Benign meningioma	Right anterior clinoid process
M6	Female	52.2	Biopsy	Benign meningioma	Left sphenoid
M7	Female	52.2	STR	Benign meningioma	Pituitary and left optic nerve sheath
M8	Male	54	STR	Benign meningioma	Left superior sagital sinus

Patient	Gender	Initial dose (Gy)	Extent of surgery	Histology	Tumor location
M9	Female	50.4	Biopsy	Benign meningioma	Right posterior fossa
M10	Male	50.4	STR	Benign meningioma	Left petroclival region
P1	Male	52.2	STR	Pituitary adenoma	Pituitary
P2	Female	50.4	STR	Pituitary adenoma	Pituitary
P3	Male	45	STR	Pituitary adenoma	Pituitary

GTR gross total resection, *STR* subtotal resection

Table 2

Mean doses to the NPC-containing structures with non-sparing versus sparing radiation techniques for the non-NPC-sparing and NPC-sparing RT plans in the mouse model

Structure	Mean dose (Gy) Non-NPC sparing	Mean dose (Gy) NPC sparing
Ipsilateral LV	5.2	1.2
Contralateral LV	2.5	0.04
Ipsilateral DG	2.8	0.08
Contralateral DG	3.3	0.02

Values are from Monte Carlo dose calculations

Table 3

Mean reduction in dose received by 70% (D70) of the contralateral DG and contralateral lateral ventricle in the human retrospective planning study with NPC-sparing IMRT plans compared with the conventional IMRT plans

Patient	*n*	Contralateral DG		Contralateral lateral ventricle	
		Δ (Gy)	Δ (%)	Δ (Gy)	Δ (%)
GBM	10	8.3 (7.0 to 14.3)	35.9 (6.0 to 75.1)	7.3 (2.5 to 13.4)	35.9 (10.7 to 63.7)
Low-grade glioma	10	1.8 (−0.15 to 5.42)	11.7 (−0.3 to 65.0)	4.2 (−0.5 to 10.4)	19.6 (−1.0 to 42.0)
Meningioma	10	1.2 (−1.46 to 7.28)	10.5 (−4.5 to 58.0)	3.7 (0.43 to 7.02)	41.4 (13.5 to 74.6)
Pituitary	3	0.5 (−0.4 to 1.27)	2.3 (−2.0 to 5.0)	5.61 (2.0 to 8.34)	64.74 (56.8 to 70.5)